Progress In Electromagnetics Research C, Vol. 105, 217–227, 2020

Small Signal Bi-Period Harmonic Undulator Free Electron Laser

Ganeswar Mishra*, Avani Sharma, and Saif M. Khan

Abstract—In this paper, we discuss the spectral property of radiation of an electron moving in a bi-period harmonic undulator field with a phase between the primary undulator field and the harmonic field component. We derive the expression for the photons per second per mrad^2 per 0.1% BW of the radiation. A small signal gain analysis also is discussed highlighting this feature of the radiation. A bi-period index parameter, i.e., Λ is introduced in the calculation. According to the value of the index parameter, the scheme can operate as one period or bi-period undulator. It is shown that when $\Lambda = \pi$, the device operates at the fundamental and the third harmonic. However, when $\Lambda = \pi/2$, it is possible to eliminate the third harmonic.

1. INTRODUCTION

Insertion devices are the key components of the synchrotron radiation and free electron laser sources. There are interests and technology upgrades of undulator technology for synchrotron radiation source (SRS) and free electron laser (FEL) for producing tunable electromagnetic radiation over the desired electromagnetic spectrum [1–12]. In the synchrotron radiation source, the relativistic electron beam propagates in the magnetic undulator field and emits spontaneous radiation. In the free electron laser scheme, the relativistic electron beam exchanges the kinetic energy to a co-propagating radiation field at the resonant frequency. Most insertion devices are undulators designed either as pure permanent magnet or hybrid permanent magnet according to Halbach field configuration. The modern synchrotron and free electron laser facilities have undertaken key technology upgrades for the undulator to provide superior spectral and gain qualities enabling experiments in a variety of disciplines and applications. The resonant frequency of the synchrotron radiation source or the free electron laser is tuned via electron beam energy or the undulator period or the undulator magnetic field strength. The energy tuning is associated with the accelerator technology and the complicated difficult task of focusing and trajectory issue in the undulator magnets. The energy tunability in free electron lasers is supplemented by two-stream schemes. An alternative way of wavelength is tuning the variation of the field amplitude via gap variations [13]. The wavelength tuning via variation of the field amplitude is an issue in long undulators using x ray free electron laser. The field amplitude in the long undulator of the x ray free electron laser requires precision better than 0.1% in different undulator sections of the beam line. Adjustment of the gaps of all undulator sections with such high precision is a technological issue. The synchrotron radiation source and free electron laser performance have been upgraded by the use of a step tapered undulator. The scheme of the step tapered undulator alters the resonance condition halfway through the undulator [14–16]. A step tapered undulator provides two independently tunable resonances, and a two-color operation is feasible similar to two-stream free electron laser or two-stream electron cyclotron resonance maser [17–21]. A third possibility exists in the changing mechanism of the undulator periods. The period length of the installed operational undulator provides an easy technological tool to the tuning of radiation wavelength without interrupting the accelerator and the gap precision [22–30].

Received 22 May 2020, Accepted 10 September 2020, Scheduled 27 September 2020
* Corresponding author: Ganeswar Mishra (gmishra_dauniv@yahoo.co.in).
The authors are with the Devi Ahilya Vishwavidyalaya, Indore, Madhya Pradesh 452001, India.

For a planar type undulator with an ideal sinusoidal field profile, the electron oscillates on axis at the fundamental and its odd harmonics. Higher harmonic operation is often aimed to extend the wavelength tuning towards short wavelength with lower beam energy. Some methods such as putting high permeability shims along the undulator length have been adopted and are used. It has been demonstrated that harmonic undulators can be exploited to regulate the emission of certain selected harmonics and hence contribute to the development of the efficient devices with high extraction and narrow spectrum [31–38].

In this paper we investigate the undulator radiation with a bi-period harmonic undulator in Section 2. A small signal gain is given in Section 3. The results and discussion are discussed in Section 4. In our scheme, we assume that the third harmonic radiation is built by putting high permeability shims along the length of the undulator. We consider a phase between the two field components of the harmonic undulator. It is shown in the calculation that the phase between the two field components introduces a bi-period index parameter in the undulator radiation and small signal gain expression. Accordingly when the bi-period harmonic undulator index parameter equals an integral multiple of π, the device operates as a bi-period device, i.e., at the fundamental and third harmonic. However when the parameter equals $\pi/2$, it is possible to eliminate the third harmonic.

2. BI-PERIOD HARMONIC UNDULATOR RADIATION

We consider the on axis magnetic field of the bi-period harmonic undulator which consists of the primary field and its third harmonic field component. Accordingly, we represent the magnetic field as,

$$\vec{B} = [0,\ \{B_1 \sin(k_u z) + B_3 \sin(3k_u z + \varphi)\}\,\hat{y},\ 0] \tag{1}$$

where $k_u = 2\pi/\lambda_u$, λ_u is the undulator period. B_1 and B_3 are the two field amplitudes. φ is the phase associated with the third harmonic magnetic field. The velocity and trajectory can be found from the Lorentz force equation,

$$\beta_x = -\frac{K}{\gamma}\left[\cos\left(k_u z\right) + \delta_3 \cos\left(3k_u z + \varphi\right)\right] + \theta_x \tag{2}$$

where $K = eB_1/m_0 c k_u$ is an undulator parameter and $\delta_3 = B_3/3B_1$. In Eq. (3), we assume imperfect trajectory with angular incidence as $\theta_x = \beta_x(0)/\beta_z(0)$. From the energy conservation, we get the longitudinal electron velocity as,

$$\begin{aligned}
\beta_z &= \beta^* - \frac{K^2}{4\gamma^2}\left[\cos 2\omega_u t + \delta_3^2 \cos 2\left(3\omega_u t + \varphi\right)\right] + \frac{K\theta_x}{\gamma}\left[\cos \omega_u t + \delta_3 \cos(3\omega_u t + \varphi)\right] \\
\beta^* &= 1 - \frac{1}{2\gamma^2}\left\{1 + \frac{K^2}{2}\left(1 + \delta_3^2\right) + \gamma^2\theta_x^2\right\}
\end{aligned} \tag{3}$$

A further integration gives the electron trajectories as

$$\begin{aligned}
x &= -\frac{cK}{\gamma\omega_u}\left[\sin\left(\omega_u t\right) + \frac{\delta_3}{3}\left\{\sin\left(3\omega_u t + \varphi\right) - \sin\varphi\right\}\right] \\
z &= \beta^* ct - \frac{cK^2}{8\gamma^2\omega_u}\left[\sin 2\omega_u t + \frac{\delta_3^2}{3}\left\{\sin 2\left(3\omega_u t + \varphi\right) - \sin 2\varphi\right\}\right] \\
&\quad + \frac{c\theta_x K}{\gamma\omega_u}\left[\sin \omega_u t + \frac{\delta_3}{3}\left\{\sin\left(3\omega_u t + \varphi\right) - \sin\varphi\right\}\right]
\end{aligned} \tag{4}$$

The brightness is the energy per unit solid angle per unit angular frequency is evaluated from the Lienard-Wiechert potential.

$$\frac{d^2 I}{d\omega d\Omega} = \frac{e^2\omega^2}{16\pi^3\varepsilon_0 c}\left|\int_{-\infty}^{+\infty}\left\{\hat{n} \times (\hat{n} \times \vec{\beta})\right\}\exp\left[i\omega\left(t - \frac{z}{c}\right)\right] dt\right|^2 \tag{5}$$

where $\hat{n}$ is a unit vector determining the direction of observation and ω is the emission frequency. e is the electronic charge. $\vec{\beta}$ is the normalized velocity. c is the velocity of light. The integration is carried out over the interaction length. The triple vector product in Eq. (5) is simplified to

$$\{\hat{n} \times (\hat{n} \times \vec{\beta})\}_x = \frac{K}{\gamma}\left[\cos\left(k_u z\right) + \delta_3 \cos\left(3k_u z + \varphi\right)\right] - \theta_x \tag{6}$$

The exponential term in Eq. (5) reads

$$\exp\left[i\omega\left(t - \frac{z}{c}\right)\right] = \sum_{m,n} J_m\left(\xi_1, \xi_2\right) J_n\left(\xi_{3a}, \xi_{3b}\right) \exp\left[i\left(\xi_{3a}\sin\varphi + \xi_{3b}\sin 2\varphi - n\varphi\right)\right] \exp\left(i\nu t\right) \tag{7}$$

where the detuning parameter υ is defined as,

$$\nu = \omega_u^*\left[\frac{\omega}{2\gamma^2\omega_u^*}\left(1 + \frac{K^2\left(1+\delta_3^2\right)}{2} + \gamma^2\theta_x^2\right) - \omega_u^*\right], \qquad \omega_u^* = m\omega_u + n(3\omega_u) \tag{8}$$

where $J_m\left(\xi_1, \xi_2\right)$ are $J_n\left(\xi_{3a}, \xi_{3b}\right)$ the Generalized Bessel Functions (GBF). The arguments of the GBFs are

$$\xi_1 = \frac{\omega\theta_x K}{\gamma\omega_u}, \quad \xi_2 = -\frac{\omega K^2}{8\gamma^2\omega_u}$$

$$\xi_{3a} = \frac{\omega\theta_x K_1}{\gamma\omega_u}\frac{\delta_3}{3}, \quad \xi_{3b} = -\frac{\omega K^2}{8\gamma^2\omega_u}\frac{\delta_3^2}{3}$$

Substituting $\hat{n} \times (\hat{n} \times \vec{\beta})$ and phase term in the brightness expression in Eq.? (5) and integrating over the limit 0–T where $T = \frac{N_u\lambda_u}{c\beta_z}$, N_u is the number of undulator periods, we get

$$\frac{d^2 I}{d\omega d\Omega} = \frac{e^2\omega^2 T^2}{64\pi^3\varepsilon_0 c\gamma^2} JJ_{mn}^2 \cos^2\Lambda \frac{\sin^2(\nu/2)}{(\nu/2)^2} \tag{9}$$

where $\Lambda = \xi_{3a}\sin\varphi + \xi_{3b}\sin 2\varphi - n\varphi$ and the coupling constant JJ_{mn} in Eq. (9) are given in terms of generalized Bessel functions (GBF) as

$$\begin{aligned} JJ_{mn} = {} & K\left[\left\{J_{m+1}\left(\xi_1, \xi_2\right) + J_{m-1}\left(\xi_1, \xi_2\right)\right\} J_n\left(\xi_{3a}, \xi_{3b}\right)\right. \\ & \left. + \delta_3\left\{J_{n+1}\left(\xi_{3a}, \xi_{3b}\right) + J_{n-1}\left(\xi_{3a}, \xi_{3b}\right)\right\} J_m\left(\xi_1, \xi_2\right)\right] - 2\gamma\theta_x J_m\left(\xi_1, \xi_2\right) J_n\left(\xi_{3a}, \xi_{3b}\right) \end{aligned} \tag{10}$$

The radiation frequency is obtained at the resonance condition i.e., $\upsilon = 0$ given by

$$\omega = \frac{2\gamma^2\left(\omega_u^*\right)}{1 + \frac{K^2(1+\delta_3^2)}{2} + \gamma^2\theta_x^2} \tag{11}$$

where m and n are the harmonic integers of radiations at ω_u and $3\omega_u$ frequencies, respectively.

Substituting the value of ω from Eq. (11) in Eq. (9) and simplifying, we get the following equation

$$\frac{d^2 I}{d\omega d\Omega} = \frac{e^2\gamma^2 N_u^2\left(\omega_u^*\right)^2}{4\pi\varepsilon_0 c\omega_u^2} F_{mn}(K)\cos^2\Lambda \frac{\sin^2(\nu/2)}{(\nu/2)^2} \tag{12}$$

The angular energy distribution function is defined as,

$$F_{mn}(K) = \frac{m^2 JJ_{mn}^2}{\left(1 + \frac{K^2\left(1+\delta_3^2\right)}{2} + \gamma^2\theta_x^2\right)^2} \tag{13}$$

The energy emitted per electron per pass can readily be converted into an on axis angular power density by multiplying the number of electrons per second (I_b/e, where I_b is the beam current). Eq. (12) is converted to the number of photons per second, and the result can be expressed in terms of relative bandwidth $d\omega/\omega$.

$$\frac{d^2\dot{N}}{d\Omega d\omega/\omega} = \frac{e^2\gamma^2 N_u^2\left(\omega_u^*\right)^2}{4\pi\varepsilon_0 c\omega_u^2}\frac{I_b}{e}\frac{2\pi}{h} F_{mn}(K)\cos^2\Lambda \frac{\sin^2(\nu/2)}{(\nu/2)^2} \tag{14}$$

In units of photons per second per mrad^2 per 0.1% bandwidth, we get

$$\frac{d\dot{N}}{d\Omega} = 1.74 \times 10^{14} \frac{N_u^2 E^2 I_b \left(\omega_u^*\right)^2}{\omega_u^2} F_{mn}(K) \cos^2 \Lambda \frac{\sin^2(\nu/2)}{(\nu/2)^2} \tag{15}$$

3. SMALL SIGNAL FREE ELECTRON LASER GAIN

Now we calculate the small signal gain of a free electron laser with a bi-period harmonic undulator. Let us consider a radiation field as

$$\vec{E}_x(z,t) = -\widehat{x} E_0 \cos(kz - \omega t + \psi_0) \tag{16}$$

where ψ_0 is the phase of the electron with the radiation field. The change in energy of the electron is given by

$$\frac{dW}{dt} = -ec\vec{v} \cdot \vec{E}, \quad W = \gamma m_e c^2 \tag{17}$$

Eq. (3) and Eq. (16) are used to solve Eq. (18), and we obtain

$$\begin{aligned} \frac{dW}{dt} &= \frac{ecKE_0}{2\gamma} \left[\left\{ \cos\left(\psi^+ - 3k_u z - \varphi\right) + \cos\left(\psi^- + 3k_u z + \varphi\right) \right\} \right. \\ &\quad \left. + \delta_3 \left\{ \cos\left(\psi^+ - k_u z\right) + \cos\left(\psi^- + k_u z\right) \right\} \right] - eE_0 \theta_x \cos\left(kz - \omega t + \psi_0\right) \end{aligned} \tag{18}$$

where $\psi^{\pm} = (k \pm k_u \pm 3k_u)z \pm \varphi - \omega t + \psi_0$. With the substitution $\cos x = \mathrm{Re}(e^{ix})$

$$\begin{aligned} \frac{dW}{dt} &= ecE_0 \frac{K}{2\gamma} \mathrm{Re} \left[\left\{ e^{i\left(\psi^+ - 3k_u z - \varphi\right)} + e^{i\left(\psi^- + 3k_u z + \varphi\right)} \right\} + \delta_3 \left\{ e^{i\left(\psi^+ - k_u z\right)} + e^{i\left(\psi^- + k_u z\right)} \right\} \right] \\ &\quad - eE_0 \theta_x \mathrm{Re} \left\{ e^{i(kz - \omega t + \psi_0)} \right\} \end{aligned} \tag{19}$$

Eq. (20) is simplified after averaging over an undulator to find

$$\frac{dW}{dz} = \frac{ecE_0 \tilde{K}}{2\gamma} \cos(\Lambda) \cos\psi \tag{20}$$

where

$$\begin{aligned} \tilde{K} &= K\left(a_0 + \delta_3 a_1\right) - 2\gamma\theta_x a_2 \\ \psi &= (k + k_u^*)\bar{z} - \omega t + \psi_0, \quad k_u^* = mk_u + n3k_u \\ a_0 &= \left\{ J_{m+1}\left(\xi_{1a}, \xi_{1b}\right) + J_{m-1}\left(\xi_{1a}, \xi_{1b}\right) \right\} J_n\left(\xi_{3a}, \xi_{3b}\right) \\ a_1 &= \left\{ J_{n+1}\left(\xi_{3a}, \xi_{3b}\right) + J_{n-1}\left(\xi_{3a}, \xi_{3b}\right) \right\} J_m\left(\xi_{1a}, \xi_{1b}\right) \\ a_2 &= J_m\left(\xi_{1a}, \xi_{1b}\right) J_n\left(\xi_{3a}, \xi_{3b}\right) \end{aligned} \tag{21}$$

There will be continuous energy transferring from the electron to electromagnetic wave if $\psi = \text{const.}$ i.e., $\dot{\psi} = 0$. We consider $\gamma > \gamma_R$ and define $\eta = (\gamma - \gamma_R)/\gamma_R$ as the relative energy deviation. Both the energy deviation $\eta\gamma_R m_e c^2$ and the ponderomotive phase will change with the interaction with the electromagnetic wave. The time derivative of the ponderomotive phase i.e., $\dot{\psi} = 0$ is no longer zero for $\gamma > \gamma_R$. Thus we can have

$$\dot{\Psi} = k_u^* c - kc \left(1 + \frac{K^2\left(1 + \delta_3^2\right)}{2} + \gamma^2 \theta_x^2 \right) / 2\gamma^2$$

When we put $\gamma \sim \gamma_R$

$$\dot{\Psi} = 0 = k_u^* c - kc \left(1 + \frac{K^2\left(1 + \delta_3^2\right)}{2} + \gamma^2 \theta_x^2 \right) / 2\gamma_R^2 \tag{22}$$

Subtracting these two equations, Eq. (21) and Eq. (22) can be put together to read

$$\dot{\Psi} = 2k_u^* c\eta \tag{23}$$

Using Eq. (23) and Eq. (21), we develop the pendulum equation for the free electron laser as

$$\frac{d^2\psi}{dt^2} + \Omega^2 \cos\Psi = 0 \tag{24}$$

where

$$\Omega^2 = \frac{eE_0 k_u^* \tilde{K}}{m_e \gamma_R^2} \cos\Lambda \cos\varphi$$

The energy increase and the relative gain caused by the single electron is given by $\Delta W = -(\Delta\eta)\gamma_R m_e c^2$. The energy per unit volume of the electromagnetic wave is $W = \varepsilon_0 E_0^2/2$. The gain from the single electron is written as

$$G = -2\gamma_R m_e c^2 \Delta\eta / E_0^2 \varepsilon_0 \tag{25}$$

Using $\Delta\dot{\Psi} = 2k_u^* c\Delta\eta$ from Eq. (23) and by summing over all the electrons in the bunch, we rewrite the gain as,

$$G = -\frac{\gamma_R m_e c n_e}{k_u^* \varepsilon_0 E_0^2} \left\langle \Delta\dot{\psi} \right\rangle \tag{26}$$

In Eq. (26), $\langle \Delta\dot{\psi} \rangle$ denotes the change in time derivative of the ponderomotive phase averaged over all the electrons. Using Eq. (24), Eq. (26) can be written as,

$$G = -\frac{e^2 k_u^* c n_e}{\varepsilon_0 m_e \gamma_R^3 \Omega^4} \tilde{K}^2 \cos^2\Lambda \left\langle \Delta\dot{\psi} \right\rangle \tag{27}$$

The pendulum equation is solved by standard procedure to give

$$\left\langle \Delta\dot{\psi} \right\rangle = \frac{L^3 \Omega^4}{8c^3} \frac{d}{d(\nu T/2)} \left[\frac{\sin(\nu T/2)}{(\nu T/2)} \right]^2 \tag{28}$$

From Eq. (27), we get the free electron laser gain

$$G = -\frac{e^2 n_e k_u^* L^3}{8\varepsilon_0 m_e c^2 \gamma_R^3} \tilde{K}^2 \cos^2\Lambda \frac{d}{d(\nu T/2)} \left[\frac{\sin(\nu T/2)}{(\nu T/2)} \right]^2 \tag{29}$$

4. RESULTS & DISCUSSION

The resonance frequency is given in Eq. (11). The electron longitudinal motion (see Eq. (4)) gets modulated at twice of the fundamental undulator frequency and its third harmonic component, resulting in radiation at harmonics at these frequencies given by,

$$\omega = 2\gamma^2 \omega_u^* / (1 + 0.5 \times K^2(1 + \delta_3^2) + \gamma^2 \theta_x^2)$$

The expression $\omega_u^* = m\omega_u + n(3\omega_u)$ reads that the undulator radiates at frequency $\omega_u^* = m\omega_u$, where $m = 1, 3, 5, \ldots$. Higher harmonic radiation corresponding to $m = 3, 5, \ldots$ occurs in a conventional undulator with relatively larger undulator parameter. There is a need to operate the undulator device at a higher harmonic which is very much possible with lower electron beam energy. However, the higher harmonic radiations are very weak. This necessitates the introduction of additional high permeability shims inside the undulator. Arranging the shims at the periodicity of $3\omega_u$ introduces additionally harmonics through $\omega_u^* = n(3\omega_u)$, implying that the radiation at $m\omega_u (m = 3)$ and $n(3\omega_u)(n = 1)$ are superposed. This is an attractive feature of the harmonic undulator. Eq. (15) is the useful derivation to compute the photons per second per mrad^2 per 0.1% BW. It contains two modifying terms, the harmonic angular energy distribution function and the bi-period undulator index parameter. The harmonic undulator angular energy distribution function is the planar undulator angular energy distribution function with $\delta_3 = 0$. The planar undulator angular energy distribution function for the fundamental is shown in Fig. 1. The fundamental is highest at a value of the undulator parameter with $\sim K = 1$. The planar undulator angular energy distribution function for the third harmonic is shown in Fig. 2. The fundamental is highest at a value of the undulator parameter with $\sim K = 2$. The effects of the imperfect trajectory is to decrease the both. The angular distribution function for the

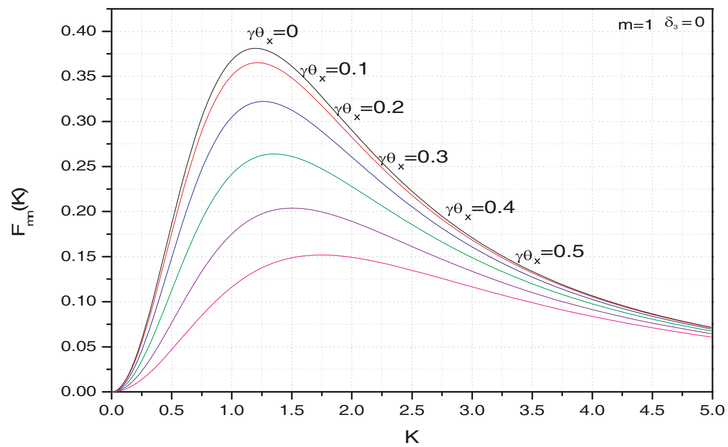

Figure 1. Angular energy density distribution function for the fundamental of the standard planar undulator.

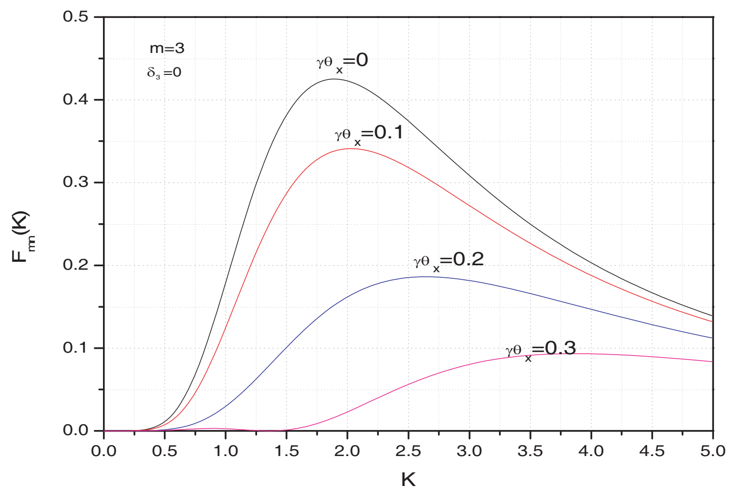

Figure 2. Angular energy density distribution function for the third harmonic of planar undulator.

harmonic undulator is plotted in Fig. 3 for the fundamental harmonic at a typical value of $\delta_3 = 0.3$. The value decreases. The third harmonic of the harmonic undulator value increases at an earlier value of the undulator parameter than the planar undulator case. Additionally, the harmonic $n = 1$ enhances the intensity at $m = 3$. Fig. 4 and Fig. 5 give the angular energy distribution function for the higher harmonics, i.e., $m = 3$, $n = 0$ and $m = 0$, $n = 1$, respectively.

The photons per second per mrad^2 per 0.1% BW is modified by $\cos^2 \Lambda$, $\Lambda = \xi_{3a} \sin\varphi + \xi_{3b} \sin 2\varphi - n\varphi$ in Eq. (15). We call this as bi-period index parameter. This term contains the integer number n, therefore associated with the additional harmonics introduced by the harmonic field components. For a perfect electron beam properly aligned with the undulator $\xi_{3a} = 0$, $\Lambda = \xi_{3b} \sin 2\varphi - n\varphi$. For $\varphi = 2\pi$, $\Lambda = \xi_{3b} \sin 4\pi - n2\pi$, $\cos^2 \Lambda = 1$. The device will operate as bi-period, and both the fundamental and third harmonic will contribute to the radiation. For $\varphi = \pi/2$, $\Lambda = n\pi/2$, $\cos^2 \Lambda = 0$. The device will operate as one period, and the third harmonic gets eliminated. In Fig. 6, we plot the harmonic undulator radiation defined by $m = 1$ and $m = 3$. The radiation at these frequencies is not affected by the phase. In Fig. 7, we plot the higher harmonic explicitly. The higher harmonic defined by $m = 3$ exists for both $\varphi = \pi, \pi/2$. The higher harmonic defined by $n = 1$ survives for the case $\varphi = \pi$ but gets eliminated at $\varphi = \pi/2$. This is most desirable finding of this manuscript. By a proper phase selection, the additional third harmonic intensity can be added more than 50 percent (see Fig. 7).

The small signal gain of the harmonic undulator is defined in Eq. (29). The gain is modified by

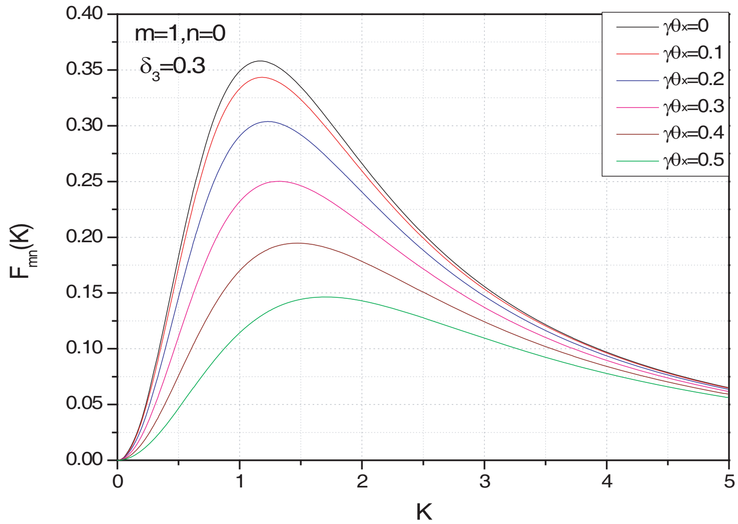

Figure 3. Angular energy distribution function for the harmonic undulator-fundamental harmonic.

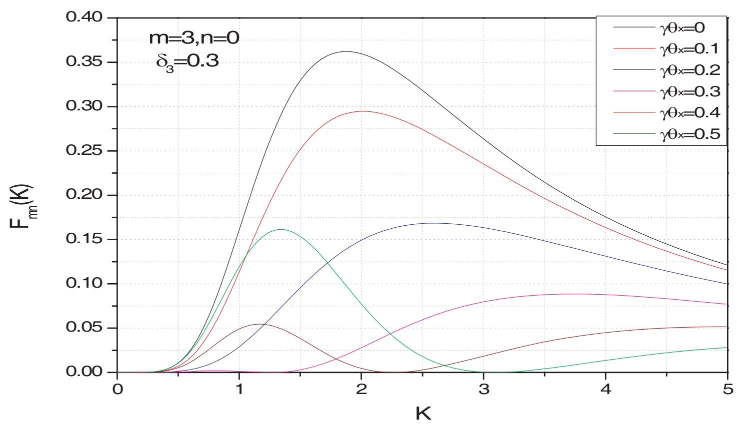

Figure 4. Angular energy distribution function for the harmonic undulator third harmonic.

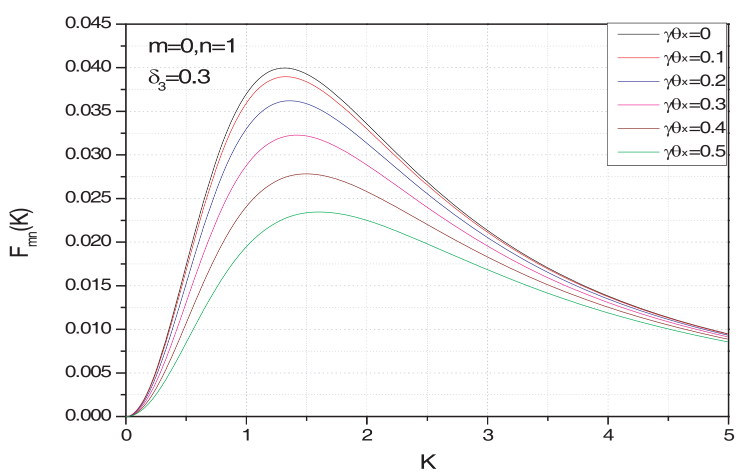

Figure 5. Angular energy distribution function for the harmonic undulator at the additional harmonic.

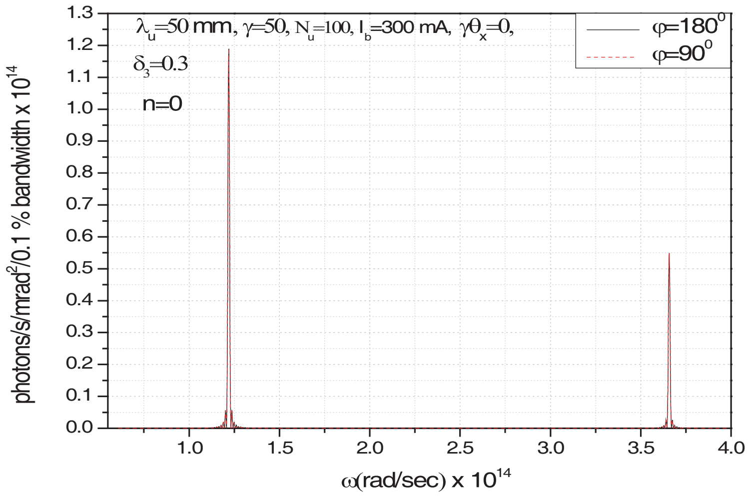

Figure 6. Harmonic undulator radiation at the fundamental and third harmonic.

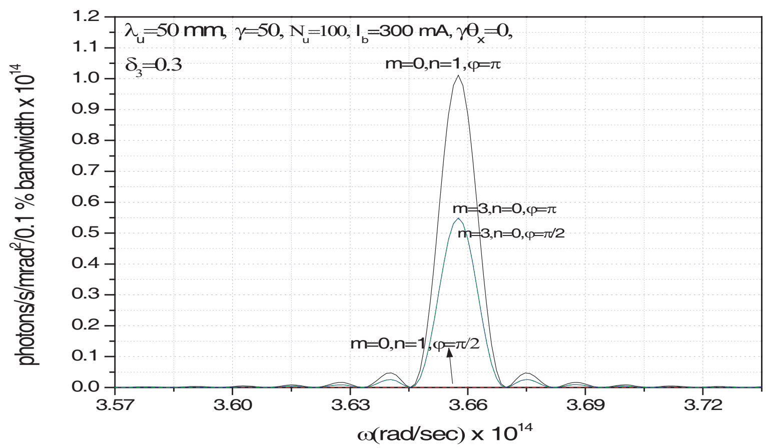

Figure 7. Harmonic undulator radiation at $m = 1$, $m = 3$ and $n = 1$.

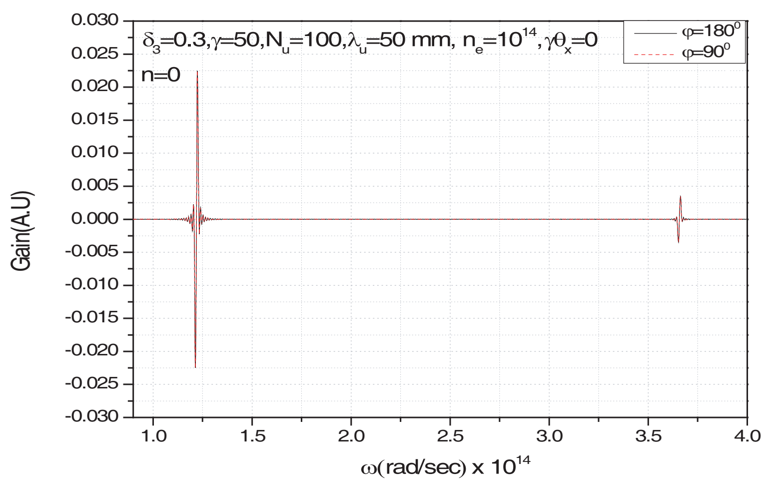

Figure 8. Small signal gain.

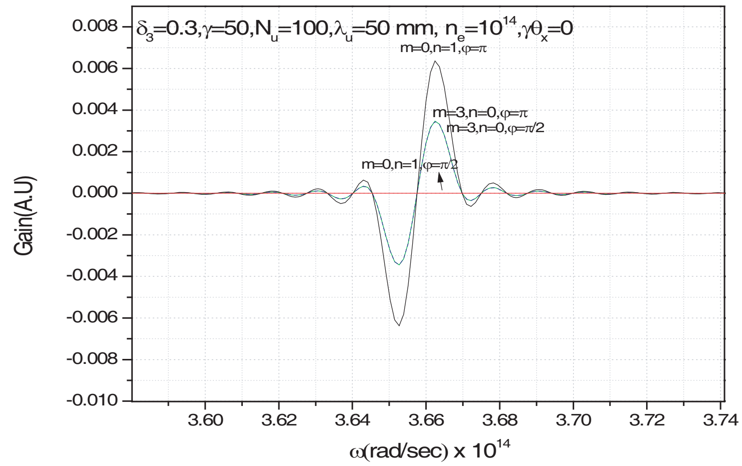

Figure 9. Small signal gain at the higher harmonic.

$\cos^2 \Lambda$. This property on the small signal gain is illustrated in Fig. 8 and Fig. 9, respectively. The gain at higher harmonic defined by $n = 1$ survives for the case $\varphi = \pi$ and contributes to higher gain but gets eliminated at $\varphi = \pi/2$.

ACKNOWLEDGMENT

This work is financially supported by SERB, Delhi Govt of India through a grant No. CRG/ 2018/00849.

REFERENCES

1. Seddon, E. A., J. A. Clarke, D. J. Dunning, C. Masciorecchio, C. J. Miline, F. Parmigiani, R. Dugg, J. C. H. Spence, N. R. Thompson, K. Udea, S. M Vinko, J. S. Wark, and W. Wurth, "Short wavelength free electron laser sources and science: A review," *Reports on Progress in Physics*, Vol. 80, No. 11, 115901, 2017.
2. Huang, C. S., J. C. Jan, C. S. Chang, S. D. Chen, C. H. Chang, and T. M. Ven, "Development trends for insertion devices for future light sources," *Phy. Rev. Spl. Topics — Accl. & Beams*, Vol. 14, 044801, 2017.
3. Pellegrini, C., "X-ray free electron lasers: From dreams to reality," *Physica Scripta*, Vol. T169, 014004, 2017.
4. Rossbach, J., J. R. Schneider, and W. Wurth, "10 years of Pioneering x-ray science at the free electron laser FLASH at DESY," *Physics Reports*, Vol. 808, 1–74, 2019.
5. Dattoli, G., E. Di Palma, S. Pagnutti, and E. Sabia, "Free electrón coherent sources: From microwave to X rays," *Physics Reports*, Vol. 739, 1–52, 2018.
6. Tanaka, T., "Current status and future prospective of accelerator based x-ray light source," *Journal of Optics*, Vol. 19, No. 9, 2017.
7. Gaith, A., D. Oumbarek, and M. E. Couprie, "Tunable high spatio spectral purity undulator radiation from a transported laser plasma accelerated electron beam," *Scientific Reports*, Vol. 9, 19020, 2019.
8. Couprie, M. E., "Undulator technologies for future free electron laser facilities and storage rings," *Proceedings of IPAC*, 29–30, MOZB102, Shanghai, China, 2013.
9. Yamamoto, S., "Development of very short period undulators," *9th International Particle Accelerator Conference, IPAC 2018*, 1845–1847, Jacow Publishing, Vancouver, B.C, Canada, 2018.
10. Ji, F., R. Chang, Q. Zhou, W. Zhang, M. Ye, S. Sasaki, and S. Qiao, "Design and performance of the APPLE knot undulator," *Journal of Synchrotron Radiation*, Vol. 22, Part 4, 901, 2015.

11. Kitamura, H., "Recent trends of insertion device technology for X-ray sources," *Journal of Synchrotron Radiation*, Vol. 7, Part 3, 121, June 2000.
12. Huang, J. C., H. Kitamura, C. K. Yang, and C. H. Chang, "Challenges of in vacuum and cryogenic permanent magnet undulator technologies," *Phys. Rev. Accl. Beams. — Accl. & Beams*, Vol. 20, 064801, 2017.
13. Heung, S., K. Kang, and H. Loos, "X ray free electron laser tuning for variable gap undulator," *Phys. Rev. Accl. Beams*, Vol. 22, No. 6, 060703, 2019.
14. Jaroszynski, D. A., R. Prazers, F. Glotin, and J. M. Ortega, "Two colour operation of the free electron laser using a step tapered undulator," *Nuclear Instruments and Methods in Physics Research, A*, Vol. 358, No. 1–3, 224–227, 1995.
15. Blau, J., V. Bouras, W. B. Colson, K. Polykandriotis, A. Kalfoutzos, S. V. Bcnson, and G. R. Neil, "Simulation of the 100 KW TJNAF FEL using step tapered undulator," *Nuclear Instruments and Methods in Physics Research A*, Vol. 483, 138–141, 2002.
16. Peng, L., Z. Yang, and S. Liu, "Dual undulator free electron laser," *Optics Communication*, Vol. 98, Nos. 4–6, 285, 1993.
17. Mahadizadeh, N., "Efficiency enhancement in a two stream free electron laser with a helical wiggler," *Optik*, Vol. 182, 1170, 2019.
18. Kulish, V. V., A. Lysenko, and V. I. Savchenko, "Two stream free electron laser: General properties," *International Journal of Infrared and Millimeter Waves*, Vol. 24, No. 2, 129, 2003.
19. Marinelli, A., D. Ratner, A. Lutman, J. Turner, J. welch, F. J. Decker, H. Loos, C. Behrens, S. Gilevich, A. A. Miahnahri, S. Vetter, T. J. Maxwell, Y. Ding, R. Coffe, S. Wakatsuki, and Z. Huang, "High intensity double pulse x ray free electron laser," *Nature Communications*, Vol. 6, 6369, 2015.
20. Bekefi, G., "Double stream cyclotron maser," *Nuclear Instruments and Methods in Physics Research A*, Vol. 318, 243, 1992.
21. Saviz, S., Z. Rezaei, and F. M. Aghamir, "Gain enhancement in two-stream free electron laser with a planar wiggler and an axial guide magnetic field," *Chin. Phys. B*, Vol. 21, No. 9, 094103, 2012.
22. Davidyuk, I. V., O. A. Shevchenko, V. G. Tcheskidov, N. A. Vinokurov, and Ya. V. Getnamov, "Developing an undulator with a variable period for the first stage of Novosibirsk free electron laser," *Bulletin of the Russian Academy of Science: Physics*, Vol. 83, No. 2, 155–158, 2019.
23. Davidyuk, I. V., "Modelling and designing of variable period and variable Pole number undulator," *Phy. Rev. Accl. Beams*, Vol. 19, 020701, 2016.
24. Vinokurov, N. A., O. A. Shevchenko, and V. G. Tcheskidov, "Variable period permanent magnet undulators," *Phys. Rev. Spl. Topics — Accl. & Beams*, Vol. 14, 040701, 2011.
25. Meseck, A., J. Bahrdt, W. Frentrup, M. Huck, C. Kuhn, R. Rethfeldt, M. Scheer, amd E. Rial, "Tripple period undulator," *10th International Particle Accelerator Conference, IPAC 2019*, TUPRB022, Australia, 2019.
26. Su, C. H. and C. H. Chang, "Designing and multi staggered array undulator," *IEEE Trans. Applied Superconductivity*, Vol. 14, No. 2, 576–579, 2004.
27. Shenoy, G. K., J. W. Lewellen, D. Suha, and N. A. Vinukurov, "Variable period undulators as synchrotron radiation sources," *J. Synchrotron Radiation Sources*, Vol. 10, 205, 2003.
28. Mun, J., Y. U. Jeong, N. A. Vinokurov, K. Lee, K. H. Jang, S. H. Park, M. Y. Jeon, and S. I. Shin, "Variable period permanent magnet helical undulator," *Phys. Rev. Spl. Topics — Accl. & Beams*, Vol. 17, 080701, 2014.
29. Ramm, T. and M. Tischer, "Development of a revolver type undulator," *Proceedings of the 10th Mechanical Engineering Design of Synchrotron Radiation Equipment and Instrumentation*, TUPH3, Paris, France, 2018.
30. Tanaka, T. and H. Kitamura, "Composite period undulator to improve the wavelength tunability of free electron lasers," *Phys. Rev. Spl. Topics — Accl. & Beams*, Vol. 15, 050701, 2011.
31. Jia, Q., "Effects of undulator harmonics field on free electron laser harmonic generation," *Phy. Rev. Spl. Topics — Accl. & Beams*, Vol. 14, 060702, 2011.

32. Zhuovsky, K. V. and A. M. Kalitenko, "Harmonics generation on Planar undulators in single pass free electron lasers," *Russian Physics Journal*, Vol. 62, No. 2, 354–362, 2019.
33. Zhukovsky, K. V., I. A. Potapov, and A. M. Kaliterko, "Two-frequency undulators for generation of x-ray radiation in free electron lasers," *Quantum Electronics*, Vol. 61, No. 3, 216–231, 2018.
34. Zhukovsky, K., "Two frequency undulator in a short SASE FEL for angstrom wavelengths," *Journal of Optics*, Vol. 20, No. 9, 2018.
35. Dattoli, G., V. V. Mikhalin, P. L Ottaviani, and K. V. Zhukovsky, "Two frequency undulator and harmonic generation by an ultra relativistic electron," *Journal of Applied Physics*, Vol. 100, No. 8, 084507–084507-12, 2006.
36. Zhukovsky, K. and I. Potapov, "Two frequency undulator usage in compact self amplified spontaneous emission free electron laser in Ranentgen range," *Laser and Particle Beams*, Vol. 35 No. 2, 325–336, 2017.
37. Jeevakhan, H. and G. Mishra, "Spectral properties of two frequency harmonic undulator radiation and effect of energy spread," *Nuclear Instruments and Methods in Physics Research*, Vol. 656, No. 1, 101, 2011.
38. Mishra, G., M. Gehlot, and H. Jeevakhan, "Spectral properties of bi harmonic undulator radiation," *Nuclear Instruments and Methods in Physics Research*, Vol. 603, No. 3, 495, 2009.